RSC Applied Polymers

ROYAL SOCIETY OF CHEMISTRY

PAPER

View Article Online
View Journal | View Issue

Cite this: *RSC Appl. Polym.*, 2025, **3**, 156

Preparation of 4D hydrogels with PET-RAFT and orthogonal photo-reactions†

Chanhyuk Jee,[a] Hikaru Matsumoto,[a] Tasuku Horiuchi,[a] Zaiyang Liu,[b] Zhongkui Wang,[b] Obayashi Kakeru,[c] Ken Kojio,[d] Masanori Nagao[a] and Yoshiko Miura *[a]

Received 19th July 2024,
Accepted 21st October 2024

DOI: 10.1039/d4lp00232f

rsc.li/rscapplpolym

We conducted an experiment to compare the predicted outcomes with the practical results of synthesizing four-dimensional (4D) hydrogels and observing their 4D motion. We employed a computer simulator and utilized PET-RAFT and orthogonal chemistry methods. To initiate the study on 4D materials, we employed the swelling method and controlled it by utilizing visible light synthesis. To regulate the irradiation time of blue light, we employed cinnamoyl ethyl acrylate as an orthogonal system to control crosslinking density. Various physical properties were assessed using a rheometer. Our findings confirmed that the movement could be controlled by adjusting the swelling ratio of the upper and lower parts, thereby implementing a bi-layer design based on differences in crosslinking density. This study highlights the successful synthesis of hydrogels with diverse physical properties and demonstrates the potential of 4D materials through the orthogonal synthesis technique.

1. Introduction

Four-dimensional (4D) materials change their shape and properties with time and have a variety of excellent functionalities.[1] 4D materials are smart materials that can change properties in response to the environment (temperature, humidity, light, voltage, *etc.*). Hydrogels are important 4D soft materials, which easily deform based on the swelling and shrinking properties. 4D materials with hydrogels have been studied in the fields of soft actuators[2–4] and soft robotics.[5–7] In addition, since hydrogels work as 4D materials in aqueous solutions,[8–10] they can be applied to biomaterials and biodevices.[11–13] Hydrogels exhibit 4D properties based on their swelling properties in solvents and can change the properties through variations in crosslinking density.[14–18]

Hydrogel-based 4D materials have been actively researched in the fields of both synthetic and physical chemistry. Hydrogels are usually obtained with crosslinked polymers. Although 90% of the gel's volume is water, its properties are largely influenced by the properties of crosslinked polymers. The non-uniform microstructure of the polymers leads to reduced mechanical strength and response to stimuli.[19] Therefore, there has been a demand for synthetic polymer gels with uniform and controllable polymer structures.

One method to obtain a uniform gel is the utilization of a uniform polymer. One viable method for achieving the uniform polymer is reversible deactivation radical polymerization (RDRP),[20] which enables controlled polymerization rates and suppression of undesired termination reactions for achieving controlled chain lengths. Among RDRP techniques, the combination of reversible addition-fragmentation chain transfer (RAFT) reagents[21] and photoredox catalysis, specifically electron/energy transfer-RAFT (PET-RAFT) polymerization, has garnered significant attention due to its versatility and oxygen tolerance.[22] The use of polymer gels with PET-RAFT is an important method for the preparation of 4D materials.[23]

Photopolymerization by PET-RAFT is a light-specific reaction with photocatalysts and RAFT reagents and is applicable to photo-selective reactions. PET-RAFT polymerization could be combined with other light-specific reactions, leading to photo-orthogonal reactions. Therefore, it is possible not only to perform precise photopolymerization but also to synthesize polymers with complex chemical structures by orthogonal photochemical reactions at different light wavelengths. In other words, sophisticated materials can be created by combining orthogonal photoreactions. Orthogonal reaction techniques have been explored for multifunctional and precisely

[a]*Department of Chemical Engineering, Graduate School of Engineering, Kyushu University, 744 Motooka, Nishi-ku, Fukuoka, 819-0395, Japan. E-mail: miuray@chem-eng.kyushu-u.ac.jp*
[b]*Department of Robotics, Ritsumeikan University, Kusatsu 525-8577, Japan*
[c]*Department of Applied Chemistry, Graduate School of Engineering, Kyushu University, 744 Motooka, Nishi-ku, Fukuoka, 819-0395, Japan*
[d]*Institute for Materials Chemistry and Engineering, Kyushu University, 744 Motooka, Nishi-ku, Fukuoka 819-0395, Japan*

†Electronic supplementary information (ESI) available: Synthesis of monomers, RAFT reagents and physical properties of hydrogels. See DOI: https://doi.org/10.1039/d4lp00232f

controllable hydrogels.[22,24] However, these orthogonal reactions have not been utilized for the preparation of 4D hydrogel materials.[25,26]

In this study, we investigated the preparation of hydrogels using orthogonal photoreactions (Fig. 1). Our aim was to create stimuli-responsive hydrogel materials with controlled swelling ratios using orthogonal reactions *via* PET-RAFT polymerization and orthogonal reactions to precisely control the polymer scaffold structure and various mechanical properties by manipulating irradiation time. PET-RAFT polymerization of *N*,*N*-dimethylacrylate (DMAAm), polyethylene glycol diacrylate (PEGDA),[23] and cinnamoyl ethyl acrylate (CEA)[27–29] was performed using a RAFT reagent and a photocatalyst, erythrosine B (EB). The polymerization proceeded under green light irradiation (518 nm). Subsequently, blue light (465 nm) was used to photo-crosslink the CEA units. PET-RAFT polymerization and photo-crosslinking proceed independently, resulting in photo-orthogonal reactions for controlling cross-linking density. The physical properties of hydrogels were investigated using Fourier transform infrared spectroscopy (FTIR), viscoelastic analyses, and swelling experiments. We also explored the 4D properties of the hydrogels based on differences in swelling ratios in bi-layer structured samples.[27] Shape changes of the gels were measured by monitoring and compared based on computer-aided simulations. This method presents an intriguing approach for material formation using gels and is proposed as a method for synthesizing 4D gels.

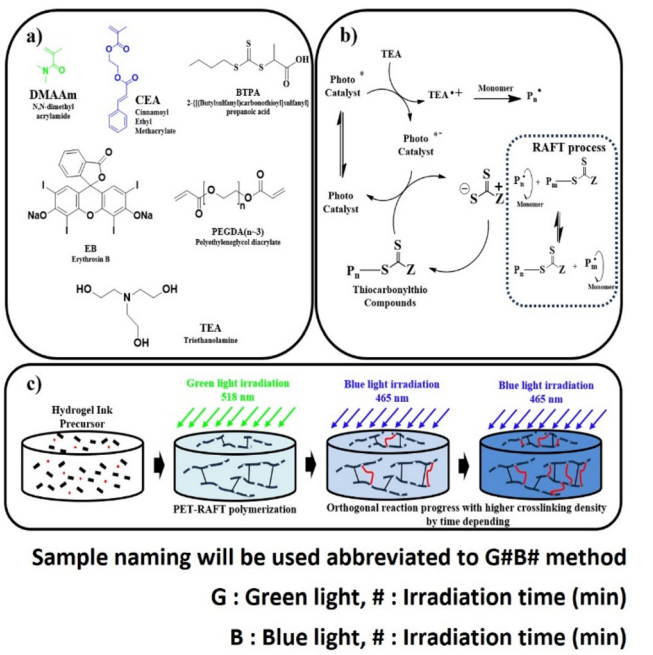

Fig. 1 Preparation of hydrogels by photo-orthogonal reactions including PET-RAFT polymerization and photo-crosslinking. (a) Chemical structures of monomers and PET-RAFT reagents, (b) mechanism of PET-RAFT polymerization, and (c) schematic of hydrogel formation by photo-orthogonal reactions.

2. Experimental

2.1. Materials

DMAAm (98%), PEGDA (n = 1–4) and EB were purchased from TCI Co. (Tokyo, Japan). Triethanolamine (TEA, 98.0%) was purchased from Merck-Aldrich (Burlington, MA, US). DMAAm was purified using an alumina column before use. Water used was purified using a Milli-Q system. CEA and 2{[(butylsulfanyl) carbonothioyl] sulfanyl} propanoic acid (BTPA) were synthesized (ESI†).[23,24] Green (NLUD05(G)-DC) and blue (NLUD05(B)-DC) LEDs from the NLUD-RGB series were purchased from Nikkiso Co., Ltd (Tokyo, Japan). The LED intensity was measured using an optical power meter (Newport Co., CA, USA).

2.2. Hydrogels from PET-RAFT polymerization and orthogonal reactions

The gel precursor solution was prepared by dissolving DMAAm (4.98 mM), CEA (25 mM), BTPA (0.3 mM), EB (0.3 mM), and TEA (100 mM) as a matrix, photo-orthogonal units, RAFT reagent, photocatalyst, and reductant, respectively, in water ([DMAAm]/[CEA]/[PEGDA]/[BTPA]/[EB]/[TEA] = 99.5 : 0.5 : 0.5 : 0.005 : 0.005 : 2). The reaction mixture was poured into a mold (11 mm in diameter) of round shape (200 μl), which was irradiated with green light (518 nm) in a box at constant temperature (25 °C) for various times (0.5–60 min), resulting in gel formation (abbreviated as **G0.5–G60**) (Fig. 1 (bottom), Scheme 1). For the second photoreaction, **G15** was subsequently irradiated with blue light (465 nm) for various times (0–30 min), resulting in orthogonally photo-crosslinked gels (abbreviated as **G15B0–G15B30**).

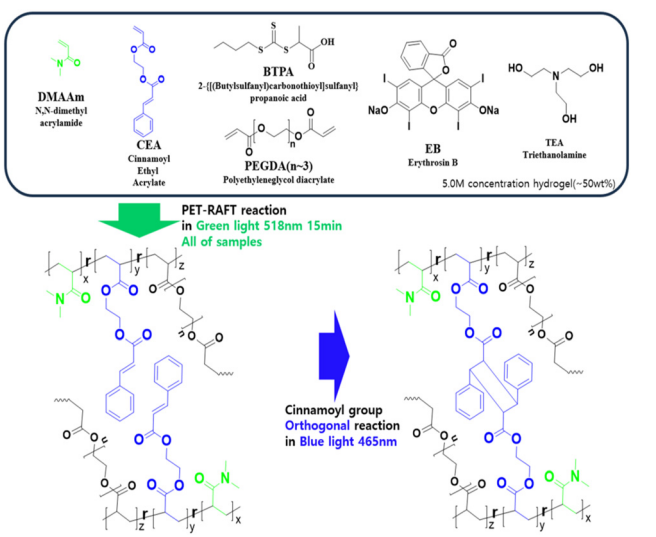

Scheme 1 Photo-orthogonal reactions *via* PET-RAFT polymerization (green light, 518 nm) and photo-crosslinking of CEA (blue light, 465 nm).

3 Characterization of the prepared PET-RAFT hydrogel samples

3.1 Attenuated total reflectance Fourier transform infrared (ATR-FTIR) spectroscopy

ATR-FTIR spectroscopy was performed to monitor using an FT/IR-4700 ATR-FTIR spectrometer (Jasco Co., Tokyo, Japan) with an ATR ZnSe crystal lens plate. Transmittance spectra were obtained by scanning the samples from 400 to 4000 cm^{-1} to monitor conversions in PET-RAFT polymerization under green light and CEA photo-crosslinking under blue light.

3.2 Frequency sweep analysis

For modulus measurement, a hydrogel was prepared with a cylindrical shape with 11 mm diameter and different thicknesses (2 and 4.5 mm). The viscoelastic modulus was evaluated using a Physica MCR 101 rheometer (Anton Paar GmbH, Graz, Austria) in frequency sweep mode in the angular frequency range of 0.1–500 rad s^{-1}. Shear strain and temperature were set to 10% and 25 °C, respectively.

3.3 Swelling ratio analysis[30,31]

The hydrogel sample was dried under vacuum for 72 hours before swelling experiments. The dried sample was first weighed and subsequently immersed in water. The sample was taken out of the water, and the weight of the swollen gels was measured at various times. The swelling ratio was calculated using the following equation:

$$\text{Swelling ratio} = \frac{(\text{measured weight of sample})\,(\text{g})}{(\text{reference sample weight})\,(\text{g})}$$

3.4 Differential scanning calorimetry (DSC) analysis

The hydrogel sample was dried by freeze–drying for 24 hours. The dried sample was first weighed for analysis by DSC using an X-DSC7000 (HITACHI, Tokyo, Japan). The analysis conditions are −30 to 100 °C with 10 °C min^{-1}.

4. Results and discussion

4.1. Preparation of hydrogels by PET-RAFT polymerization (green light)

The ATR-FTIR spectra were recorded to evaluate the polymerization progress for gel formation (Fig. 2). Peaks at 1423 cm^{-1} (CH_2 bending of CH_2═CH) and 1640 cm^{-1} (C═O vibration, DMAAm) gradually diminished (from **G0.5** to **G2**) and finally disappeared at an irradiation time of longer than 4 min. At the same time, the peak at 1618 cm^{-1} (C═O vibration, carbonyl of polymerized acrylate) remarkably increased after the irradiation of green light. These changes in ATR-FTIR spectra suggested the successful polymerization of DMAAm and PEGDA by PET-RAFT polymerization, where the conversions of monomers were controlled by irradiation of green light.[29]

The peak at 1595 cm^{-1} (N–H vibration of DMAAm) disappeared (from **G0.5** to **G2**), but nearby peaks, such as the one at 1610 cm^{-1}, increased dramatically, which caused the 1595 cm^{-1} peak to be covered, making it difficult to observe any changes.

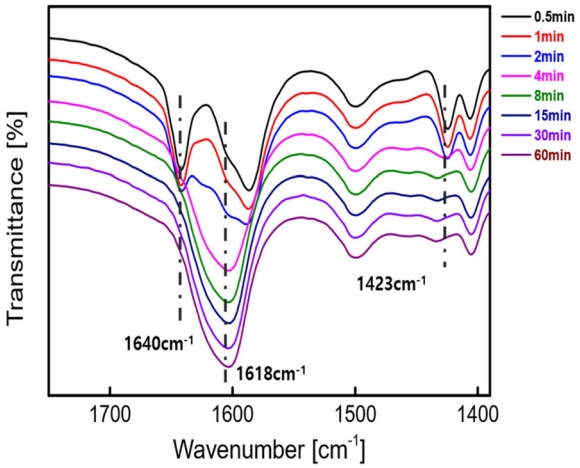

Fig. 2 ATR-FTIR spectra of the hydrogels under irradiation of green light for various irradiation times (0.5–60 min, **G0.5–G60**).

4.2. Photo-crosslinking of CEA units in hydrogels (blue light)

Having confirmed the successful control of gelation of hydrogels with green light irradiation (518 nm) by PET-RAFT polymerization, photo-crosslinking *via* irradiation with blue light was conducted.[27–29] The viscoelastic properties of **G15** after irradiation with blue light (465 nm) were investigated by dynamic mechanical analyses using a rheometer with a frequency sweep (Fig. 3). The storage modulus of the hydrogels increased with increasing irradiation time until 5 min. On the other hand, the storage modulus no longer changed after 5 min or more (Fig. 3a). The shear modulus and crosslink density were calculated for **G15B5–G15B30** (ESI, Table S1†). The loss modulus of the hydrogels showed a complex trend compared to the storage modulus (Fig. 3b). At low frequencies, most of the samples exhibited an increasing trend with the time, and angular frequency response increased with the blue light irradiation.

The samples subjected to blue light irradiation showed slight relaxation in the low-frequency region. This was probably due to relaxation of the entanglement of polymer chains. With increasing irradiation time with blue light, the terminal flow behaviours of the hydrogels in the low-frequency region shifted to lower frequencies. This shift suggests that the relaxation events were hindered by the increased crosslinking points, which suggested dimerization of CEA units *via* irradiation of blue light.

Conversely, the trend of the loss modulus is totally complicated (Fig. 3b). During the early periods of the irradiation of blue light, the storage modulus increased with the irradiation time. With further prolonged irradiation, the crosslinking density of loosened parts increases due to the orthogonal reaction. Initially, the low-density crosslink molecular structure

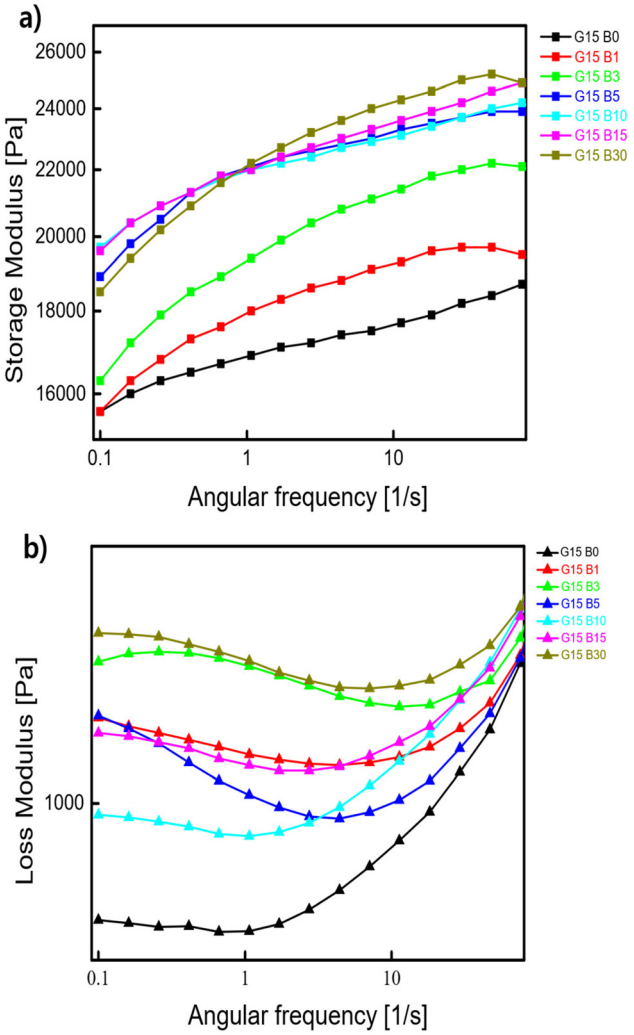

Fig. 3 (a) Storage modulus and (b) loss modulus of **G15** irradiated with blue light for various times in angular frequency sweep mode.

gradually transforms into a high-density crosslink molecular structure, impacting the storage modulus properties. The increasing crosslink density resulting from the orthogonal reaction induced by blue irradiation leads to the formation of a highly complex molecular structure, contributing to the intricate behaviour observed in the loss modulus in this study.

Typically, this trend is related to the material approaching the glass transition, where molecular motion increases in this frequency range, leading to a rise in the loss shear modulus. The loss shear modulus generally represents energy dissipation. The molecular structure of the polymer can influence the modulus trend, either increasing or decreasing it. In particular, glass transition structures and rubbery structures on a molecular scale can contribute to energy dissipation in polymer materials. Therefore, we can explain the behaviour of our hydrogel samples by attributing the increase in the loss shear modulus at low frequencies to the activation of motion in the glass transition region, which can be analysed and observed through this increase.[32] This explanation for the correlation between glass transition temperature (T_g) and crosslinking density also allows for rheological analysis.[33] Samples with higher T_g have a higher crosslinking density, and therefore we can expect the samples to behave in a rubbery or plastic-like manner. The DSC analyses are shown in ESI (Fig. S6†).

4.3. Swelling properties and 4D motions of the hydrogels

The swelling properties of the hydrogels were evaluated. The time course of the swelling ratio of a reference hydrogel, which was prepared without CEA (**G15**: green light = 15 min and blue light = 0 min), exhibited fast swelling, which reached 8.15 within 3 days. On the other hand, the swelling of a series of hydrogels was slower than that of the reference hydrogel and the swelling ratio was 5.53 within 3 days. When irradiated with blue light for 1 and 30 min, the hydrogel decreased the swelling ratio to 5.07 and 4.57 after 3 days, respectively. Long irradiation with blue light promoted photo-crosslinking of CEA units, resulting in high crosslinking density and thus a low swelling ratio. The high crosslinking density inhibited the penetration of water through the network of the hydrogels.

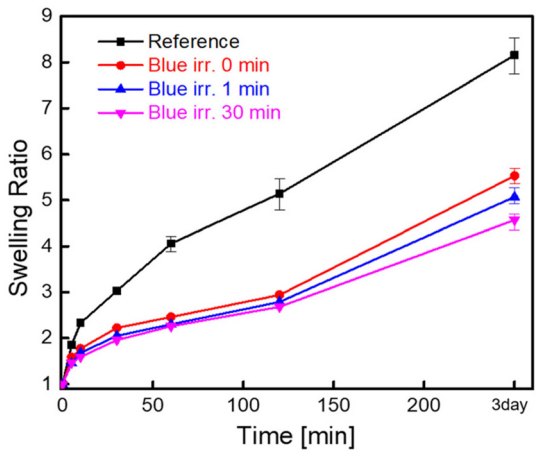

Fig. 4 The swelling ratios of the hydrogels irradiated with blue light for different irradiation times (gel prepared in the absence of CEA (reference), **G15B0**, **G15B1**, and **G15B30**).

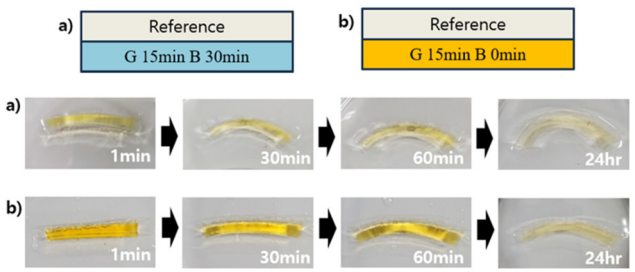

Fig. 5 4D motions of bi-layer-structured hydrogels composed of (a) **G15B30** + reference hydrogel and (b) **G15B0** + reference hydrogel upon immersion in water for different times. The size of each hydrogel layer = 25 mm × 5 mm × 2 mm.

Table 1 Swelling ratios of hydrogels irradiated with blue light for various times

	0 min	5 min	10 min	30 min	60 min	120 min	3 days
PEGDA0.5/CEA0.5 **G15B0**	1	1.58	1.77	2.22	2.46	2.94	5.53
PEGDA0.5/CEA0.5 **G15B1**	1	1.45	1.68	2.05	2.30	2.79	5.07
PEGDA0.5/CEA0.5 **G15B30**	1	1.46	1.59	1.96	2.26	2.68	4.57
Reference hydrogel	1	1.85	2.33	3.03	4.06	5.14	8.15

From the swelling properties of the hydrogels after blue light irradiation, it was confirmed that the photo-crosslinking was successfully achieved and controllable, where CEA units acted as effective cross-linkable points *via* activation using blue light irradiation. This photo-orthogonal strategy would provide smart 4D materials by designing hydrogels with different mechanical properties.

Based on the swelling properties of the hydrogels, we envisaged that the combination of different swelling properties of hydrogels would enable 4D motions in water. Bilayer structures were designed using hydrogel bars with different crosslinking degrees. One hydrogel bilayer was composed of the reference hydrogel (upper side) and **G15B30** (Fig. 5a). To our delight, this combination exhibited drastic changes in its whole shape (bending angle = 36°) by larger deformation of the reference hydrogel (upper side) than that of **G15B30** (lower side) (Fig. 4 and 5a). (The bending angle definition is in the ESI†). Surprisingly, the hydrogel bilayer composed of the reference hydrogel (upper side) and **G15B0** showed less deformation (bending angle = 21°) (Fig. 5b), explained by the small difference of the swelling ratios of the hydrogels (Fig. 4). From these observations, the 4D motions of the bi-layer structured hydrogels can be designed based on differences in swelling ratios between the layers. Furthermore, it is noteworthy that the swelling properties of the hydrogels can be easily tuned by photo-orthogonal reactions under visible light, allowing users to select their wavelength by changing the chemistries of photocatalysts and photo-cross linkable points (Table 1).

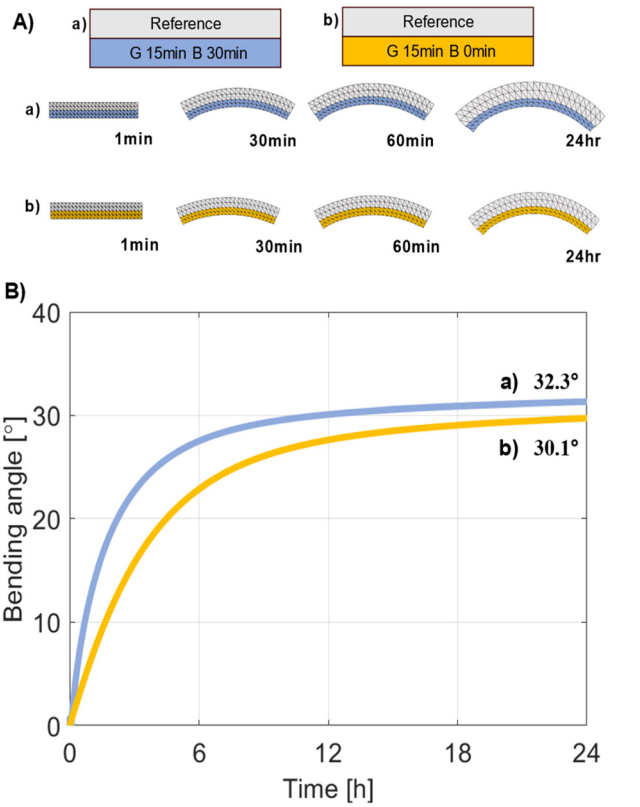

Fig. 6 Computer simulation of 4D motions of hydrogel bi-layers of (a) **G15B30** + reference hydrogel and (b) **G15B0** + reference hydrogel in (A). (B) The simulated changes in the bending angles of the hydrogel bi-layer.

4.4. Computer simulations of 4D motions of bi-layer hydrogels

The 4D motions of the hydrogel bi-layers were calculated using their swelling kinetics (Fig. 6). We constructed finite element models for deformation of each layer to predict changes in bending angles.[34,35] The model used 200 triangles for meshing for computational efficiency and accuracy. Because the gel underwent large deformations, we included geometric non-linearity in our simulations to more accurately model the gel's behaviour. Our simulations revealed that the gel bends towards the side with the lower swelling ratio. It was noteworthy that the different swelling ratios between the layers caused the bending mainly in the *x*–*z* plane, while those in the *x*–*y* and *y*–*z* planes could be ignored. The bi-layer system of **G15B30** (Fig. 5A) showed a bending angle of 32.3° (Fig. 5B), while that of the **G15B0** system was 30.1°. Although the trend of simulated bending angles was the same as those of experimental results, there was no difference in the quantitative degree of bending differences in swelling ratios between the layers, which developed changes in the bending angle, as explained by computer simulations. This insight is crucial for designing bi-layer hydrogels as 4D materials in underwater applications.

5. Conclusions

We have developed a novel method for controlling 4D hydrogels through photo-orthogonal reactions. The hydrogel was synthesized *via* PET-RAFT polymerization under green light irradiation. Additionally, the cross-linking degree of the hydrogel was regulated by the irradiation time of blue light, which induced the dimerization of the cinnamoyl groups as photo-crosslinked points. Rheological analysis of the hydrogel

revealed that the viscoelasticity depended on the irradiation time of visible light. In swelling experiments, the bi-layer hydrogels exhibited 4D motions, the bending angle of which depended on the difference in swelling ratios of each layer. Computer simulations suggested their applicability in predicting the 4D motions of hydrogels based on the input of their physical properties. The photo-orthogonal reactions highlighted the potential for controlling the mechanical properties and 4D motions of smart hydrogels. While smart 4D hydrogels are gaining attention in the field of soft materials, methods for controlling physical properties and local modifications remain challenging. In this sense, photo-orthogonal reactions are versatile and present a promising avenue for advances in sophisticated 4D materials. Hydrogel design using precise photoreactions, such as photo-orthogonal reactions, is an important aspect in the development of precise soft matter. We believe that the concept of photochemical reactions we have presented here, together with 3D printers, will play an important role in the future of 4D material design.

Author contributions

C. Jee, T. Horiuchi, and Y. Miura designed the experiments. C. Jee and T. Horiuchi performed the experiments. C. Jee, H. Matsumoto and Y. Miura wrote the manuscript. Z. Liu and Z. Wang performed the calculation of 4D movement. C. Jee, K. Obayashi, and K. Kojio performed the measurements of hydrogel rheological properties. All authors approved the final version of the manuscript.

Data availability

The authors confirm that the data supporting the findings of this study are available within the article and its ESI.†

Conflicts of interest

There are no conflicts to declare.

Acknowledgements

This article is based on results obtained from a project, JPNP14004, commissioned by the New Energy and Industrial Technology Development Organization (NEDO).

References

1 Y. Dong, S. Wang, Y. Ke, L. Ding, X. Zeng, S. Magdassi and Y. Long, *Adv. Mater. Technol.*, 2020, **5**, 2000034.
2 M. Ding, L. Jing, H. Yang, C. E. Machnicki, X. Fu, K. Li, I. Y. Wong and P. Y. Chen, *Mater. Today Adv.*, 2020, **8**, 100088.
3 Q. Shi, H. Liu, D. Tang, Y. Li, X. Li and F. Xu, *NPG Asia Mater.*, 2019, **11**, 64.
4 J. Wei, R. Li, L. Li, W. Wang and T. Chen, *Nano-Micro Lett.*, 2022, **14**, 282.
5 Z. Shen, F. Chen, X. Zhu, K. T. Yong and G. Gu, *J. Mater. Chem. B*, 2020, **8**, 8972–8991.
6 Y. Zhao, M. Hua, Y. Yan, S. Wu, Y. Alsaid and X. He, *Annu. Rev. Control. Robotics Auton. Syst.*, 2022, **5**, 515–545.
7 W. Sun, S. Schaffer, K. Dai, L. Yao, A. Feinberg and V. W. Wood, *Front. Robot. AI*, 2021, **8**, 673533.
8 Y. W. Lee, H. Ceylan, I. C. Yasa, U. Kilic and M. Sitti, *ACS Appl. Mater. Interfaces*, 2021, **13**, 12759–12766.
9 M. Neumann, G. D. Marco, D. Iudin, M. Viola, C. F. Nostrum, B. G. P. Ravensteijn and T. Vermonden, *Macromolecules*, 2023, **56**, 8377–8392.
10 Y. W. Lee, J. K. Kim, U. Bozuyuk, N. O. Dogan, M. T. A. Khan, A. Shiva, A. M. Wild and M. Sitti, *Adv. Mater.*, 2023, **35**, 2209812.
11 Y. Jian, B. Wu, X. Yang, Y. Peng, D. Zhang, Y. Yang, H. Qiu, H. Lu, J. Zhang and T. Chen, *Supramol. Mater.*, 2022, **1**, 100002.
12 Y. W. Lee, S. Chun, D. Son, X. Hu, M. Schneider and M. Sitti, *Adv. Mater.*, 2022, **34**, 2109325.
13 H. M. E. Husseiny, E. A. Mady, L. Hamabe, A. Abugomaa, K. Shimada, T. Yoshida, T. Tanaka, A. Yokoi, M. Elbadawy and R. Tanaka, *Mater. Today Bio*, 2022, **13**, 100186.
14 H. Yuk, S. Lin, C. Ma, M. Takaffoli, N. X. Fang and X. Zhao, *Nat. Commun.*, 2017, **8**, 14230.
15 R. Liang, L. Wang, H. Yu, A. Khan, B. U. Amin and R. U. Khan, *Eur. Polym. J.*, 2019, **114**, 380–396.
16 A. Kawamura, *Polym. J.*, 2017, **49**, 751–757.
17 H. Shigemitsu and I. Hamachi, *Acc. Chem. Res.*, 2017, **50**, 740–750.
18 W. M. Gramlich, I. L. Kim and J. A. Burdick, *Biomaterials*, 2013, **34**, 9803–9811.
19 T. Sakai, T. Matsunaga, Y. Yamamoto, C. Ito, R. Yoshida, S. Suzuki, N. Sasaki, M. Shibayama and U. I. Chung, *Macromolecules*, 2008, **41**, 5379–5384.
20 K. Matyjaszewski, *Macromolecules*, 2020, **53**, 495–497.
21 G. Moad, E. Rizzardo and S. H. Thang, *Chem. – Asian J.*, 2013, **8**, 1634–1644.
22 J. Phommalysack-Lovan, Y. Chu, C. Boyer and J. Xu, *Chem. Commn.*, 2018, **54**, 6591–6606.
23 Z. Zhang, N. Corrigan, A. Bagheri, J. Jin and C. Boyer, *Angew. Chem., Int. Ed.*, 2019, **58**, 17954–17963.
24 H. Wei, M. Lei, P. Zhang, J. Leng, Z. Zheng and Y. Yu, *Nat. Commun.*, 2021, **12**, 2082.
25 H. Wei, M. Lei, P. Zhang, J. Leng, Z. Zheng and Y. Yu, *Nat. Chem.*, 2011, **3**, 925–931.
26 K. Jung, N. Corrigan, M. Ciftci, J. Xu, S. E. Seo, C. J. Hawker and C. Boyer, *Adv. Mater.*, 2020, **32**, 1903850.
27 A. A. Hyder and K. S. V. Srinivasan, *J. Macromol. Sci., Part A: Pure Appl.Chem.*, 1995, **32**, 1985–1995.
28 R. Zheng, G. Liu and T. C. Jao, *Polymer*, 2007, **48**, 7049–7057.
29 S. I. Yusa, M. Sugahara, T. Endo and Y. Morishima, *Langmuir*, 2009, **25**, 5258–5265.

30 M. N. I. Shiblee, K. Ahmed, M. Kawakami and H. Furukawa, *Adv. Mater. Tech.*, 2019, **4**, 1900071.
31 J. Tang, T. Katashima, X. Li, Y. Mitsukami, Y. Yokoyama, N. Sakumichi, U. Chang, M. Shibayama and T. Sakai, *Macromolecules*, 2020, **53**, 8244–8254.
32 Hevin and P. Menard, *Dynamic Mechanical Analysis. A practical Introduction*, 2nd edn, 2008..
33 L. E. Nielsen, *J. Macromol. Sci., Part C: Polym. Rev.*, 1969, **3**, 69–103.
34 M. Kameoka, Y. Watanabe, M. N. I. Shiblee, M. Kawakami, J. Ogawa, A. Khosla, H. Furukawa, S. Zhang, S. Hirai and Z. Wang, *Machines*, 2023, **11**, 103.
35 Z. Wang, T. Hirata, T. Sato, M. Mori, M. Kawakami, H. Furukawa and S. Kawamura, *IEEE Robot. Autom. Lett.*, 2021, **6**, 2139–2146.